Accepted Manuscript

Benzophenone based fluorophore for selective detection of Sn2+ ion: Experimental and theoretical study

Amol G. Jadhav, Suvidha S. Shinde, Sandip K. Lanke, Nagaiyan Sekar

Please cite this article as: Amol G. Jadhav, Suvidha S. Shinde, Sandip K. Lanke, Nagaiyan Sekar , Benzophenone based fluorophore for selective detection of Sn2+ ion: Experimental and theoretical study. The address for the corresponding author was captured as affiliation for all authors. Please check if appropriate. Saa(2016), doi: 10.1016/j.saa.2016.11.051

Benzophenone based fluorophore for selective detection of Sn^{2+} ion: experimental and theoretical study

Amol G. Jadhav, Suvidha S. Shinde, Sandip K. Lanke, Nagaiyan Sekar*

Department of Intermediate and Dyestuff Technology

Institute of Chemical Technology (Formerly UDCT),

N. P. Marg, Matunga, Mumbai - 400 019.

Maharashtra, India.

Email: n.sekar@ictmumbai.edu.in, nethi.sekar@gmail.com

Tel.: +22 3361 1111/ 2707; Fax: +22 3361 1020

Mumbai-400 019

Abstract:

Synthesis of novel benzophenone-based chemosensor is presented for the selective sensing of Sn^{2+} ion. Screening of competitive metal ions was performed by competitive experiments. The specific cation recognition ability of chemosensor towards Sn^{2+} was investigated by experimental (UV−visible, fluorescence spectroscopy, ^1H NMR, ^{13}C NMR, FTIR and HRMS) methods and further supported by Density Functional Theory study. The stoichiometric binding ratio and binding constant (K_a) for complex is found to be 1:1 and 1.50×10^4, respectively. The detection limit of Sn^{2+} towards chemosensor was found to be 0.3898 ppb. Specific selectivity and superiority of chemosensor over another recently reported chemosensor is presented.

Keywords: Benzophenone, Schiff base, Chemosensor, ESIPT, Sn^{2+}.

1. Introduction:

Chemosensors provide a powerful method for the efficient detection of trace metal ions and thus they have wide applications in biological [1], environmental [1], clinical [2], industrial [2] and chemical processes [1,2]. Among the various sensing techniques [3], fluorescence chemosensors [4] have been a focus of utmost importance in recent years due to their high sensitivity and selectivity [5], operational simplicity [6], rapid response time [7], and for their potential application [8] in environmental and medicinal research [9−11]. Also fluorescence chemosensing technique is more cost efficient than traditional methods such as

atomic absorption spectroscopy [12], inductively coupled plasma-mass spectrometry and inductively coupled plasma-atomic emission spectrometry [13].

Tin is involved in most of reactions during preparation of important molecules of PGF derivatives [14], coumarin derivatives [15], indole derivatives [16] and graphene sheets [17]. Tin is an essential trace mineral for humans and is found in the greatest amounts in most of the organs [18]. Some toxic effects of tin which are limited mostly to gastrointestinal is reported [19]. There are some evidences that tin is involved in cancer prevention [20]. Therefore, the development of more selective and sensitive fluorescent sensors for detection of Sn^{2+} is urgent. Structure analogs of L [21] is reported having sensitivity to Al^{3+} ion is reported. However, there are very few reports which include Sn^{2+} complexation affecting optical properties of 4-arylvinyl-2,6-di(pyridine-2yl)pyrimidines [22] and detection of Sn^{2+} ion along with Al^{3+} [23], but our sensor (L) is only selective for Sn^{2+} ion without any interference of other competitive ions.

Schiff bases (imines) and their derivatives containing fluorescent scaffold are claimed to be encouraging tools for optical sensing of metal ions [24–28]. Benzophenone derivatives have been widely used as an important chemical entity in developing materials such as photoreactive micro particles [29], hybrid photoreactive silica nanoparticles [30,31] and efficient pH sensors [32]. Some of Schiff base chemosensor showed one or more drawbacks in terms of real applicability including synthetic difficulties, fluorescence quenching, and cross-sensitivities with other competitive metal ions [33]. Hence, it is worthwhile to overcome for a practical fluorescent sensor for selective detection of metal ions like Sn^{2+}.

In this study, we report the synthesis of a new turn-on fluorescent sensor (L) that can selectively detect Sn^{2+} ion. The sensing behavior of L to various metal ions (Ba^{2+}, Cu^{2+}, Pb^{2+}, Hg^{2+}, Mn^{2+}, Ni^{2+}, Fe^{3+}, Na^{+}, Al^{3+}, Ca^{2+} and Mg^{2+}) was studied by absorption and fluorescence spectra. Moreover, sensing sites was investigated by spectroscopic techniques which is supported by DFT (Density Functional Theory).

2. Experimental

2.1 Materials and methods

All the analytical grade chemicals and reagents were procured from SD Fine Chemical Ltd. (Mumbai, India) and were used without further purification. The reactions were

monitored by thin layered chromatography (TLC) using 0.25 mm E-Merck silica gel 60 F254 pre coated plates, which were visualized with UV light. ^{1}H NMR and ^{13}C NMR spectra were recorded on a 500 MHz and 125 MHz instrument of Agilent Technology, respectively. Chemical shifts are expressed in 1 (ppm) using TMS as an internal standard. IR spectra were recorded on JASCO FTIR 4100 spectrometer within the region of 4000–450 cm^{-1}. HRMS spectral data were recorded by time of flight (TOF) method. UV–visible and Fluorescence spectra were recorded on Perkin Elmer Lambda 25 UV–VIS spectrophotometer and Varian Cary Eclipse fluorescence spectrophotometer, respectively using a quartz cell of 1-cm path length. DFT computations were performed using the Gaussian 09 (G09) program [34]. Optimized geometry of L and its complex with Sn^{2+} were carried out using B3LYP as hybrid functional and 3-21G basis set.

2.2 Synthetic scheme and characterization of L and [L+ Sn^{2+}] complex

<<Please insert Scheme1: Synthesis of (2-(2-hydroxyphenyl)-1H-benzo[d]imidazol-5-yl)(phenyl) methanone (**L**)>>

The compounds 1 and 2 were prepared by the reported procedure [35,36].

Synthesis of (2-(2-hydroxyphenyl)-1H-benzo[d]midazole-5-yl)(phenyl) methanone (**L**)
2 (3-amino, 4-hydroxybenzophenone) (1mmol) and commercially available **3 (**4-(N,N-diethylamino)-2-hydroxybenzaldehyde) (1mmol) was dissolved in ethanol. The resulting reaction mass was refluxed at 78-80°C for 2 hours (**Scheme 1**). After completion of reaction, product was precipitated by adding 25 mL of water. Precipitate formed was filtered and dried in oven at 50°C. Product was purified by recrystallization from ethanol. Yield= 72%. The synthesized compound was characterized by ^{1}H-NMR, ^{13}C NMR and HRMS analysis. M.P. = 120-122°C.

a) L ((2-(2-hydroxyphenyl)-1H-benzo[d]midazole-5-yl)(phenyl) methanone) (**Fig. S1-S4**)
^{1}H NMR (500 MHz, DMSO): δ 13.82 (s, 1H), 10.64 (s, 1H), 8.69 (s, 1H), 7.71 (d, J = 7.5 Hz, 2H), 7.68 (s, 1H), 7.64 (t, J = 7.5 Hz, 1H), 7.54 (t, J = 7.5 Hz, 2H), 7.43 (d, J = 8.3 Hz, 1H), 7.31 (d, J = 8.8 Hz, 1H), 7.02 (d, J = 8.3 Hz, 1H), 6.27 (d, J = 8.8 Hz, 1H), 6.01 (s, 1H), 3.38 (q, J = 7.0 Hz, 4H), 1.11 (t, J = 7 Hz, 6H) ppm.

^{13}C NMR (125 MHz, DMSO): δ 195.20, 172.99, 160.03, 151.26, 147.99, 141.42, 137.75, 137.18, 134.56, 132.26, 130.19, 129.82, 129.33, 128.33, 124.37, 119.32, 112.21, 104.06, 34.37, 14.82 ppm.

FT-IR: 3516 (phenolic O-H stretching), 3065 (Hydrogen bonded O-H stretching) 1650 (C=O stretch), 1615 (Imine C=N stretch), 1270 (C-N stretch) cm^{-1}.

HRMS (EI): Calcd. for $[(C_{24}H_{25}N_2O_3) = L+ H^+]$, m/z 389.1865, found m/z 389.1867.

b) $[L+ Sn^{2+}]$ complex (**Fig. S5-S8**)

^{1}H NMR (500 MHz, DMSO): δ 13.20 (s, 1H), 11.03 (s, 1H), 8.81 (s, 1H), 7.70 (d, J = 7.5 Hz, 2H), 7.68 (s, 1H), 7.65 (t, J = 7.5 Hz, 1H), 7.54 (t, J = 7.5 Hz, 2H), 7.43 (d, J = 8.3 Hz, 1H), 7.31 (d, J = 8.8 Hz, 1H), 7.03 (d, J = 8.3 Hz, 1H), 6.27 (d, J = 8.8 Hz, 1H), 6.01 (s, 1H), 3.41 (q, J = 7.0 Hz, 4H), 1.12 (t, J = 7 Hz, 6H) ppm.

^{13}C NMR (125 MHz, DMSO): δ 195.21, 180.25, 163.87, 150.02, 147.99, 141.43, 137.74, 137.19, 134.55, 132.27, 130.18, 129.83, 129.33, 128.32, 124.38, 119.31, 112.22, 104.04, 34.38, 14.81 ppm.

FT-IR: 3323 (phenolic O-H stretching), 2974 (Hydrogen bonded O-H stretching) 1665 (C=O stretch), 1613 (Imine C=N stretch), 1270 (C-N stretch) cm^{-1}.

HRMS (EI): Calcd for $[(C_{26}H_{33}N_2O_5Sn^{2+}) = L+ Sn^{2+}+ 2MeOH + H^+]$, m/z 573.1411, found m/z 573.2513.

2.3 Screening and analysis

All the cations (Ba^{2+}, Cu^{2+}, Pb^{2+}, Hg^{2+}, Mn^{2+}, Ni^{2+}, Fe^{3+}, Na^+, Al^{3+}, Ca^{2+}, Mg^{2+} and Sn^{2+}) were used in the form of their freshly prepared chloride salts. $BaCl_2$, $CuCl_2$, $PbCl_2$, $HgCl_2$, $MnCl_2.4H_2O$, $NiCl_2.6H_2O$, $FeCl_3.6H_2O$, NaCl, $AlCl_3.6H_2O$, $CaCl_2$, $MgCl_2$ and $SnCl_2.2H_2O$ salts were dissolved in water to prepare the stock solution with the concentration of 5.0 x 10^{-3} M. Similarly, L was dissolved in THF to prepare the stock solution with the concentration of 5.0 x 10^{-3} M. All the stock solutions were further diluted with THF (Tetrahydrofuran) - HEPES (2-[4-(2-hydroxyethyl)piperazin-1-yl]ethanesulfonic acid) buffer (90:10, v/v, pH 7.4) to make solutions which were used directly [37]. For the sensitivity measurement, different concentrations of Sn^{2+} ions were added to the ligand (L) solution, and the fluorescence spectra were recorded. Selectivity was checked by addition of Ba^{2+}, Cu^{2+}, Pb^{2+}, Hg^{2+}, Mn^{2+}, Ni^{2+}, Fe^{3+},

Na$^+$, Al^{3+}, Ca^{2+} and Mg^{2+} into the ligand (L) solution. The emission spectra were recorded between 445 and 650 nm by exciting the receptor at 445 nm. Excitation and emission slit width was kept at 5 nm and 10 nm, respectively. All experimental parameters were kept constant throughout in order to have precision and accuracy.

3. Results and discussion

3.1 UV–visible and fluorescence experiments

<<Please insert Fig. 1: a) Absorption spectra of L (5μM) in presence of various cations (10μM) **b)** Emission spectra of L (5μM) in presence of various cations (10μM) in THF– HEPES buffer (90:10, v/v, pH 7.4)**>>**

The optical behavior of L was initially studied using UV–Vis absorption and emission spectra in THF– HEPES buffer (90:10, v/v, pH 7.4). Absorption spectra of L (5μM) exhibited λ_{max} at 380 nm. Upon addition of Sn^{2+} ions (10μM) new strong absorption band was observed around 445 nm. On the other hand, the addition of other metal ions leads to only a weak absorption band around 445 nm clearly indicated the efficient binding of Sn^{2+} as compared to other metal ions **(Fig. 1a)**. On excitation at 445 nm, a very strong 18 fold increase (compare to L alone) in emission intensity was observed at around 488 nm for L+ Sn^{2+} while very weak (around 20-50 a.u.) emission intensity was exhibited by other metal ions complexes (L+M$^{+1/2/3}$) and L (excited at 380 nm) **(Fig. 1b)**. The fluorescence enhancement may be caused by chelation-enhanced fluorescence (CHEF) effect [38]. Alternatively, this could also be explained by inhibition of PET (Photoinduced electron transfer), ESIPT (Excited state intramolecular proton transfer) and C=N isomerization process caused enhancement in the emission [8,27,38,39].

3.2 Competitive experiments

<<Please insert Fig. 2: Competition experiment of selectivity of L towards Sn^{2+} in the presence of other cations. [L] = 5μM, [Sn^{2+}] = 10 μM, and [X^{n+}] = 10 μM in THF– HEPES buffer (90:10, v/v, pH 7.4) at λ_{exc} = 445 nm.**>>**

5

To investigate the selectivity of probe L towards Sn^{2+} in presence of other metal ions, we conducted competitive experiments. Emission intensity of ligand L (5μM) in presence of Ba^{2+}, Cu^{2+}, Pb^{2+}, Hg^{2+}, Mn^{2+}, Ni^{2+}, Fe^{3+}, Na^+, Al^{3+}, Ca^{2+} and Mg^{2+} metal ions solution (10μM) was found to be around 20-50 a.u. and identical to L alone. Upon addition of Sn^{2+} (10μM) to these solutions sufficiently strong fluorescence (12-15 fold enhancement) was observed (**Fig. 2**). The emission intensities of the resulting solution was more or less same. Hence, receptor L was shown to be a selective fluorescent sensor for Sn^{2+} in the presence of competing metal ions.

3.3 Quantitative analysis

In order to quantify the amount of Sn^{2+} ions required to bind completely to the ligand L saturation point need to be determined. Upon addition of Sn^{2+} ions from 5μM to 30μM in L (2.5 μM) solution we observed isosbestic point at around 410 nm clearly suggested the conversion of L to [L-Sn^{2+}] (**Fig. 3a**). Absorption spectra clearly suggested the formation of [L-Sn^{2+}] complex. On excitation at 445 nm [L-Sn^{2+}] complex showed increasing emission intensity at around 488 nm (**Fig. 3b**). There is no any significant increase in the emission intensity after addition of 25μM Sn^{2+} solution as saturation point has achieved. Relative fluorescence quantum yield (Φ_f) of **L** was estimated to be 0.62% in THF– HEPES buffer (90:10, v/v, pH 7.4) while that of [L-Sn^{2+}] complex is found to be 79%. Relative fluorescence quantum yields were measured using quinine sulfate in 0.1N H_2SO_4 as standard (Φ_f=0.546).

<<**Please insert Fig. 3. a)** Absorption spectra of L (2.5μM) with varying Sn^{2+} concentration in THF– HEPES buffer (90:10, v/v, pH 7.4) **b)** Fluorescence spectra of L (2.5μM) with varying Sn^{2+} concentration in THF– HEPES buffer (90:10, v/v, pH 7.4)>>

<<**Please insert Fig. 4.** Job plot (stoichiometric ratio) of L with Sn^{2+}>>

Stoichiometry of the probe (L)–analyte (Sn^{2+}) was determined by using Job's plot as continuous variation method. During this experiment the total concentration of the L and Sn^{2+}

6

was kept constant (10μM) and the mole ratios was varied for 10 different fractions. The Job's plot was obtained by plotting the fluorescence intensity (I) as a function of the mole fraction of Sn^{2+}. Complexation of L and Sn^{2+} showed 1:1 stoichiometry in **Fig. 4.**

From the fluorescence titration study, the association constant (K_a) for L-Sn^{2+} in THF–HEPES buffer (90:10, v/v, pH 7.4) was determined as $1.5 \times 10^4 \ M^{-1}$ by using Benesi-Hildebrand plot (**Fig. 5).**

<<**Please insert Fig. 5.** Benesi-Hildebrand plot>>

<<**Please insert Fig. 6.** Plot for detection limit calculation>>

Limit of Detection (LOD) was calculated from the equation LOD= (3 X SD)/slope. Fluorescence titration of the L (1μM) with Sn^{2+} was carried out by adding aliquots of Sn^{2+} from 10μM-100 μM. The standard deviation (SD) was obtained from 10 blank readings of the L (1μM). From the plot of the fluorescence intensity (I-I_o) as a function of the added Sn^{2+}, the slope was obtained. The detection limit was found to be 0.3898 ppb (**Fig. 6**).

Some known structural analogs of Ligand showing comparative sensitivity, binding constant and detection limit is given in **Table 1.** Our ligand showed specific selectivity towards Sn^{2+} ion as compare to naphtelene based ligand (Sn^{2+} and Al^{3+}). Binding constant of our ligand L ($1.50 \times 10^4 \ M^{-1}$) is quite high as compare to reported benzophenone based ligand ($5.7 \times 10^3 \ M^{-1}$).

<<**Please insert Table 1** Comparative selectivity, binding constant, detection limits with reported ligands>>

3.4 Binding sites determination

To better understand the complexation sites of receptor L with Sn^{2+}, ^1H NMR experiments were carried out in DMSO. The spectral differences are depicted in **Fig. 7**. After addition of 1.0 equivalent of Sn^{2+} salt to L in DMSO, the protons of imine and hydroxyl proton of benzophenone moiety were shifted down-field by 0.12 and 0.41 ppm, respectively while hydroxyl proton of N, N diethyl aniline moiety was shifted up-field by 0.60 ppm as compared to isolated L in DMSO. Up-field shift of hydroxyl proton indicated that acidic proton initially

available for transfer to the imine nitrogen (ESIPT) was restricted during binding of Sn^{2+} ion with expected atoms of L (Figure 7). Further addition of 2 equivalents of Sn^{2+} did not show any significant changes in the spectrum which correlated the stoichiometry ratio 1:1.

<<**Please insert Fig. 7.** Comparative changes in ^{1}H NMR of L when binds with Sn^{2+}>>

3.5 Theoretical confirmation by DFT

To get insight details of the binding sites and geometry of L during binding of Sn^{2+} to L computational calculations were performed. As expected, there is good correlation of DFT study with the experimental results as far as binding sites are concerned. Sn^{2+} binds -N atom of imine strongly having weak interactions with two Oxygen atoms of hydroxyl groups. Optimized geometry of L and L- Sn^{2+} complex has shown in **Fig. 8a-b**

<<**Please insert Fig. 8.** a) Optimized geometry of L at B3LYP/3-21g level. b) Optimized geometry of L- Sn^{2+} complex at B3LYP/3-21g level at gas phase >>

<<**Please insert Table 2** Bond lengths of selected bonds>>

Calculated bond lengths of the selected bonds are tabulated in **Table 2.** Imine (–C=N-) bond length has increased from 1.29379 Å to 1.3727 Å, both C-O bond lengths increased from 1.37598 Å to 1.44143 Å and from 1.374 Å to 1.3876 Å. Similarly, O-H bond length of benzophenone moiety has increased from 0.99423 Å to 0.99606 Å while O-H bond length of N, N diethyl aniline moiety has decreased from 0.99343 Å to 0.99134 Å which in correlation with ^{1}H NMR shift shown in **Fig. 7.**

4. Conclusion:

A simple Schiff base receptor L was synthesized for selective detection of Sn^{2+}. On complexation with Sn^{2+}, analyte L exhibited significantly distinct absorption peak at around 445 nm and pronounce increased emission intensity (18 folds) at 488 nm. The formation of complex structure by interaction of nitrogen (imine) and oxygens (phenolic group) with Sn^{2+} has been confirmed by spectroscopic techniques which was further supported by DFT study. The stoichiometric binding ratio, binding constant (K_a) and limit of detection for complex is found to

be 1:1, 1.50 x 10^4 and 0.3898 ppb, respectively. Specific selectivity to Sn^{2+}, comparable binding constant and a good limit of detection as compare to other reported chemosensor is observed.

Acknowledgements

References:

[1]   R. Martínez-Máñez, F. Sancenón, Fluorogenic and Chromogenic Chemosensors and Reagents for Anions, Chem. Rev. 103 (2003) 4419–4476. doi:10.1021/cr010421e.

[2]   J. Yao, M. Yang, Y. Duan, Chemistry , Biology , and Medicine of Fluorescent Nanomaterials and Related Systems□: New Insights into Biosensing , Bioimaging , Genomics , Diagnostics , and Therapy, Chem. Rev. 114 (2014) 6130–6178. doi:10.1021/cr200359p.

[3]   E.M. Nolan, S.J. Lippard, Tools and tactics for the optical detection of mercuric ion, Chem. Rev. 108 (2008) 3443–3480. doi:10.1021/cr068000q.

[4]   A.P. de Silva, H.Q.N. Gunaratne, T. Gunnlaugsson, A.J.M. Huxley, C.P. McCoy, J.T. Rademacher, et al., Signaling Recognition Events with Fluorescent Sensors and Switches, Chem. Rev. 97 (1997) 1515–1566. doi:10.1021/cr960386p.

[5]   J.S. Kim, D.T. Quang, Calixarene-derived fluorescent probes, Chem. Rev. 107 (2007) 3780–3799. doi:10.1021/cr068046j.

[6]   H.N. Kim, W.X. Ren, J.S. Kim, J. Yoon, Fluorescent and colorimetric sensors for detection of lead, cadmium, and mercury ions, Chem. Soc. Rev. 41 (2012) 3210. doi:10.1039/c1cs15245a.

[7]   H.N. Kim, Z. Guo, W. Zhu, J. Yoon, H. Tian, Recent progress on polymer-based fluorescent and colorimetric chemosensors., Chem. Soc. Rev. 40 (2011) 79–93. doi:10.1039/c0cs00058b.

[8]   V. Luxami, S. Kumar, ESIPT based dual fluorescent sensor and concentration dependent reconfigurable boolean operators, RSC Adv. 2 (2012) 8734–8740. doi:10.1039/c2ra21170j.

[9]   C. Kar, M. Deb Adhikari, A. Ramesh, G. Das, Selective sensing and efficient separation of Hg^{2+} from aqueous medium with a pyrene based amphiphilic ligand, RSC Adv. 2 (2012) 9201–9206. doi:10.1039/c2ra21064a.

[10]   Y. Wang, Y. Huang, B. Li, L. Zhang, H. Song, H. Jiang, et al., A cell compatible fluorescent chemosensor for Hg^{2+} based on a novel rhodamine derivative that works as a molecular keypad lock, RSC Adv. 1 (2011) 1294–1300. doi:10.1039/c1ra00488c.

[11]   D.T. Quang, J.S. Kim, Fluoro- and Chromogenic Chemodosimeters for Heavy Metal Ion Detection in Solution and Biospecimens, Chem. Rev. (2010) 6280–6301. doi:10.1021/cr100154p.

[12]   M. De la Guardia, A.R. Mauri, C. Mongay, Atomic absorption spectrometric determination of gasoline additives by vapor phase sample introduction, J. Anal. At. Spectrom. 3 (1988) 1035–1038.

[13]   W.J. McShane, R.S. Pappas, V. Wilson-McElprang, D. Paschal, A rugged and transferable method for determining blood cadmium, mercury, and lead with inductively coupled plasma-mass spectrometry, Spectrochim. Acta Part B At. Spectrosc. 63 (2008) 638–644. doi:10.1016/j.sab.2008.03.016.

[14]   M. Hamberg, B. Samuelsson, Detection and isolation of an endoperoxide intermediate in prostaglandin biosynthesis., Proc. Natl. Acad. Sci. U. S. A. 70 (1973) 899–903. doi:10.1073/pnas.70.3.899.

[15]   K.K. Upadhyay, R.K. Mishra, A. Kumar, A Convenient Synthesis of Some Coumarin Derivatives Using SnCl2 · 2H2O as Catalyst, Catal. Letters. 121 (2008) 118–120. doi:10.1007/s10562-007-9307-2.

[16]   C.S. Cho, H.K. Lim, S.C. Shim, T.J. Kim, H.J. Choi, Ruthenium-catalysed synthesis of indoles from anilines and trialkanolamines in the presence of tin(II) chloride dihydrate, Chem. Commun. 3 (1998) 995–996.

[17]   F. Li, J. Song, H. Yang, S. Gan, Q. Zhang, D. Han, et al., One-step synthesis of graphene/SnO2 nanocomposites and its application in electrochemical supercapacitors., Nanotechnology. 20 (2009) 1–5. doi:10.1088/0957-4484/20/45/455602.

[18]   M. Nath, Toxicity and the cardiovascular activity of organotin compounds: a review, Appl. Organomet. Chem. 22 (2008) 598–612. doi:10.1002/aoc.1436.

[19]   L.R. Sherman, J. Masters, R. Peterson, S. Levine, Tin Concentration in the Thymus

Glands of Rats and Mice and Its Relation to the Involution of the Gland, J. Anal. Toxicol. 10 (1986) 6–9. doi:10.1093/jat/10.1.6.

[20] Q. Wang, C. Li, Y. Zou, H. Wang, T. Yi, C. Huang, A highly selective fluorescence sensor for Tin (Sn^{4+}) and its application in imaging live cells., Org. Biomol. Chem. 10 (2012) 6740–6. doi:10.1039/c2ob25895a.

[21] S. Sinha, R.R. Koner, S. Kumar, J. Mathew, M. P. V., I. Kazi, et al., Imine containing benzophenone scaffold as an efficient chemical device to detect selectively Al^{3+}, RSC Adv. 3 (2013) 345. doi:10.1039/c2ra21967k.

[22] C. Hadad, S. Achelle, I. López-Solera, J.C. García-Martínez, J. Rodríguez-López, Metal cation complexation studies of 4-arylvinyl-2,6-di(pyridin-2-yl)pyrimidines: Effect on the optical properties, Dye. Pigment. 97 (2013) 230–237. doi:10.1016/j.dyepig.2012.12.023.

[23] S. Adhikari, S. Mandal, A. Ghosh, S. Guria, D. Das, Sn(ii) induced concentration dependent dynamic to static excimer conversion of a conjugated naphthalene derivative, Dalt. Trans. 44 (2015) 14388–14393. doi:10.1039/C5DT02146D.

[24] P.G. Cozzi, Metal-Salen Schiff base complexes in catalysis: practical aspects., Chem. Soc. Rev. 33 (2004) 410–421. doi:10.1039/b307853c.

[25] D. Pucci, I. Aiello, A. Bellusci, A. Crispini, M. Ghedini, M. La Deda, Coordination Induction of Nonlinear Molecular Shape in Mesomorphic and Luminescent Zn II Complexes Based on Salen-Like Frameworks, Eur. J. Inorg. Chem. 2009 (2009) 4274–4281. doi:10.1002/ejic.200900536.

[26] L. Wang, W. Qin, W. Liu, A sensitive Schiff-base fl uorescent indicator for the detection of Zn $^{2+}$, INOCHE. 13 (2010) 1122–1125. doi:10.1016/j.inoche.2010.06.021.

[27] D. Udhayakumari, S. Saravanamoorthy, M. Ashok, S. Velmathi, Simple imine linked colorimetric and fluorescent receptor for sensing Zn $^{2+}$ ions in aqueous medium based on inhibition of ESIPT mechanism, Tetrahedron Lett. 52 (2011) 4631–4635. doi:10.1016/j.tetlet.2011.06.097.

[28] Y. Dong, J. Li, X. Jiang, F. Song, Y. Cheng, C. Zhu, Na^+ triggered fluorescence sensors for Mg^{2+} detection based on a coumarin salen moiety, Org. Lett. 13 (2011) 2252–2255. doi:10.1021/ol200530g.

[29] M. Naddaka, E. Mondal, J. Lellouche, Preparation of novel photoreactive polycarbazole-based microparticles: Reactivity features, J. Polym. Sci. Part A Polym. Chem. 49 (2011)

4687–4693. doi:10.1002/pola.24916.

[30] A. Peled, M. Naddaka, J.-P. Lellouche, Smartly designed photoreactive silica nanoparticles and their reactivity, J. Mater. Chem. 21 (2011) 11511. doi:10.1039/c1jm00055a.

[31] A. Peled, M. Naddaka, J. Lellouche, Controllable photodeposition of metal nanoparticles on a photoreactive silica support, J. Mater. Chem. 22 (2012) 7580–7583. doi:10.1039/c2jm16785a.

[32] G. Nishimura, Y. Shiraishi, T. Hirai, A fluorescent chemosensor for wide-range pH detection., Chem. Commun. (Camb). 1 (2005) 5313–5. doi:10.1039/b508136j.

[33] M. Shyamal, P. Mazumdar, S. Maity, S. Samanta, G.P. Sahoo, A. Misra, Highly Selective Turn-On Fluorogenic Chemosensor for Robust Quantification of Zn(II) Based on Aggregation Induced Emission Enhancement Feature, ACS Sensors. 1 (2016) 739–747. doi:10.1021/acssensors.6b00289.

[34] M.J. Frisch, G.W. Trucks, H.B. Schlegel, G.E. Scuseria, M.A. Robb, J.R. Cheeseman, et al., Gaussian 09, Revision C.01, Gaussian 09, Revis. B.01, Gaussian, Inc., Wallingford CT. (2009).

[35] R. Andreozzi, M. Canterino, V. Caprio, I. Di Somma, R. Sanchirico, Salicylic Acid Nitration by Means of Nitric Acid / Acetic Acid System□: Chemical and Kinetic Characterization Abstract□:, Org. Process Res. Dev. 10 (2006) 1199–1204. doi:10.1021/op060148o.

[36] B. Gong, F. Hong, C. Kohm, L. Bonham, P. Klein, Synthesis and SAR of 2-arylbenzoxazoles, benzothiazoles and benzimidazoles as inhibitors of lysophosphatidic acid acyltransferase-β, Bioorganic Med. Chem. Lett. 14 (2004) 1455–1459. doi:10.1016/j.bmcl.2004.01.023.

[37] R. Pandey, L. Reddy, S. Ishihara, A. Dhir, V. Krishnan, Conformation induced discrimination between picric acid and nitro derivatives/anions with a Cu-pyrene array: the first decision making photonic device, RSC Adv. 3 (2013) 21365. doi:10.1039/c3ra44036b.

[38] M. Yuan, W. Zhou, X. Liu, M. Zhu, J. Li, X. Yin, et al., A multianalyte chemosensor on a single molecule: Promising structure for an integrated logic gate, J. Org. Chem. 73 (2008) 5008–5014. doi:10.1021/jo8005683.

[39] M. Yuan, Y. Li, J. Li, C. Li, X. Liu, J. Lv, et al., A colorimetric and fluorometric dual-modal assay for mercury ion by a molecule, Org. Lett. 9 (2007) 2313–2316. doi:10.1021/ol0706399.

Figures and Scheme

Fig. 1: a) Absorption spectra of L (5μM) in presence of various cations (10μM) **b)** Emission spectra of L (5μM) in presence of various cations (10μM) in THF– HEPES buffer (90:10, v/v, pH 7.4)
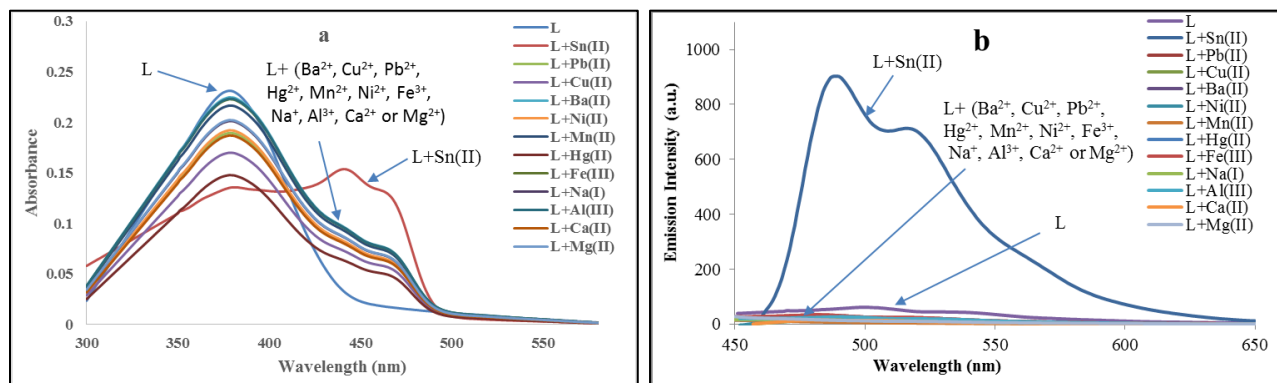
Fig. 2: Competition experiment of selectivity of L towards Sn^{2+} in the presence of other cations. [L] = 5μM, $[Sn^{2+}]$ = 10 μM, and $[X^{n+}]$ = 10 μM in THF– HEPES buffer (90:10, v/v, pH 7.4) at λ_{exc} = 445 nm.
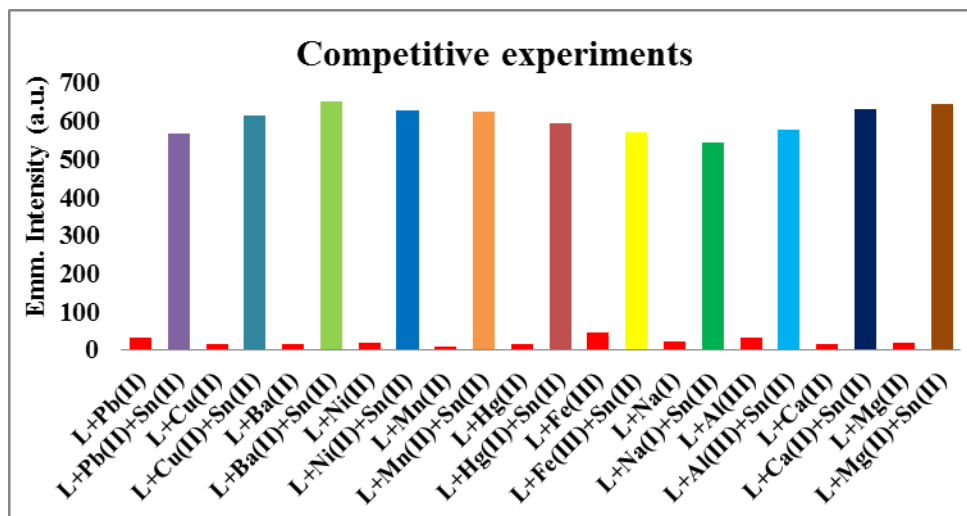
Fig. 3. a) Absorption spectra of L (2.5μM) with varying Sn^{2+} concentration in THF– HEPES buffer (90:10, v/v, pH 7.4)   **b)** Fluorescence spectra of L (2.5μM) with varying Sn^{2+} concentration in THF– HEPES buffer (90:10, v/v, pH 7.4)
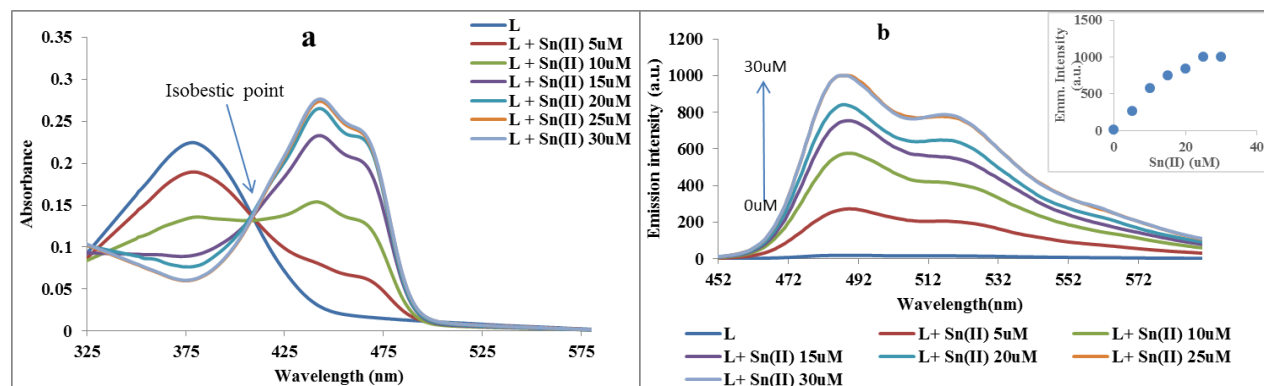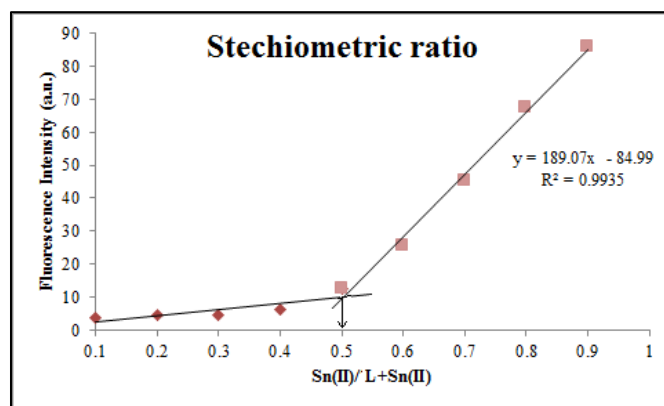
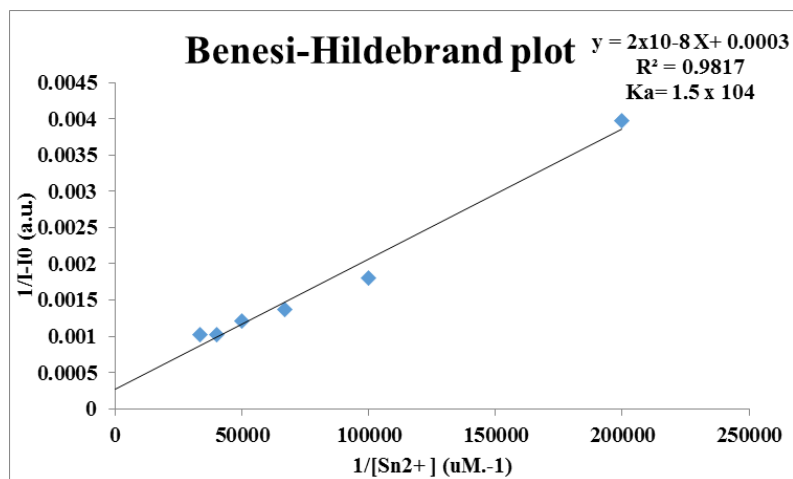**Fig. 4.** Job plot (stoichiometric ratio) of L with Sn^{2+}
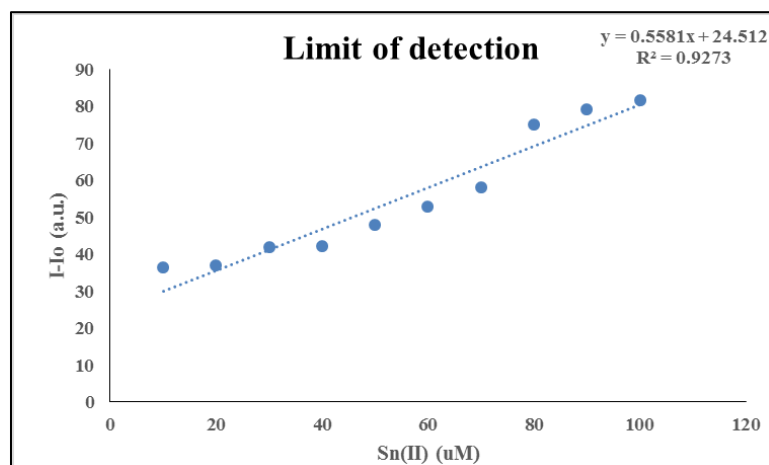
Fig. 5. Benesi-Hildebrand plot

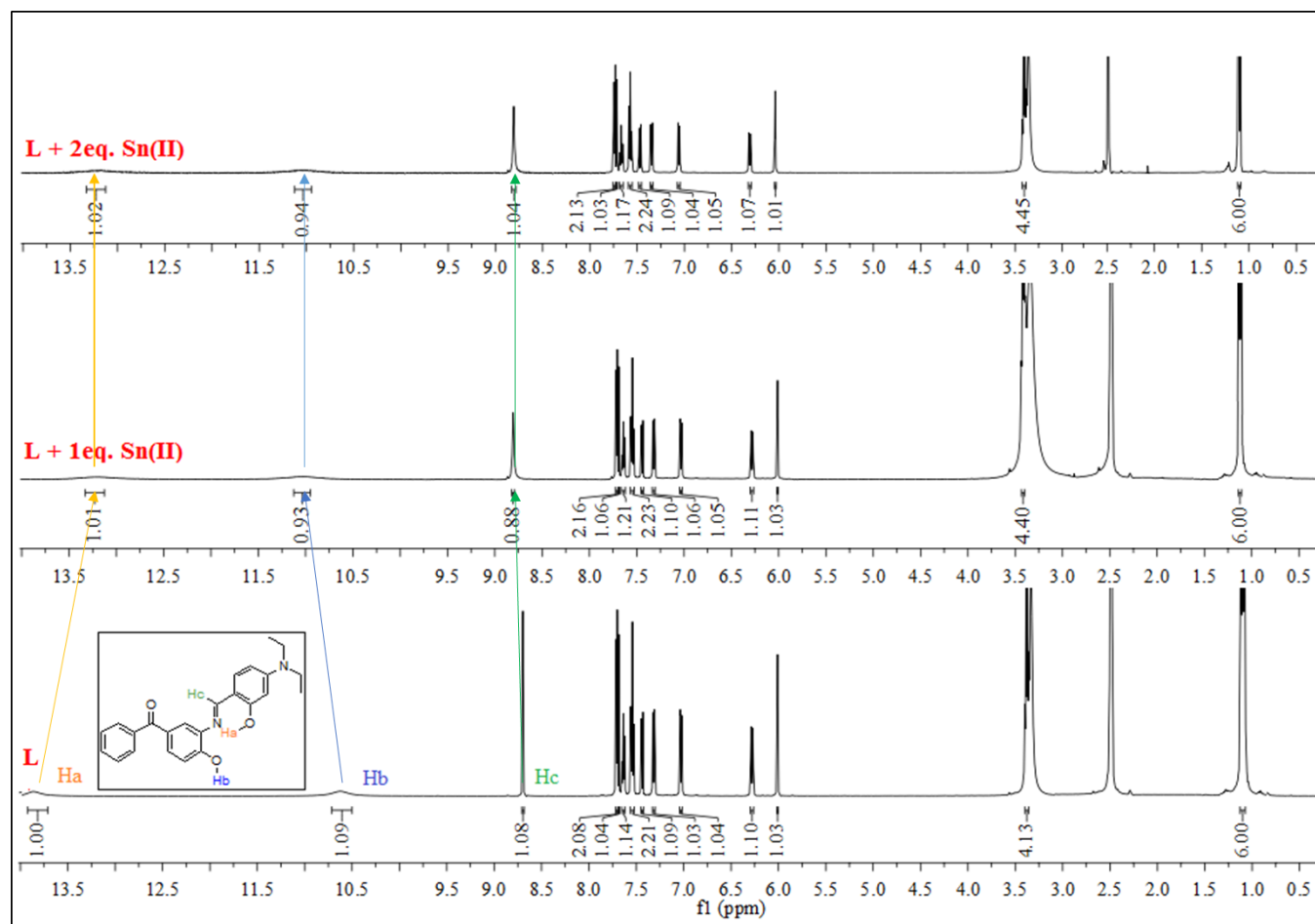**Fig. 6.** Plot for detection limit calculation

Fig. 7. Comparative changes in ^{1}H NMR of L when binds with Sn^{2+}

Fig. 8. a) Optimized geometry of L at B3LYP/3-21g level. b) Optimized geometry of L- Sn^{2+} complex at B3LYP/3-21g level at gas phase.

Scheme1: Synthesis of (2-(2-hydroxyphenyl)-1H-benzo[d]imidazol-5-yl)(phenyl) methanone (**L**)

14

Fig. 1: a) Absorption spectra of L (5μM) in presence of various cations (10μM) **b)** Emission spectra of L (5μM) in presence of various cations (10μM) in THF– HEPES buffer (90:10, v/v, pH 7.4)

Fig. 2: Competition experiment of selectivity of L towards Sn^{2+} in the presence of other cations. [L] = 5µM, $[Sn^{2+}]$ = 10 µM, and $[X^{n+}]$ = 10 µM in THF– HEPES buffer (90:10, v/v, pH 7.4) at λ_{exc} = 445 nm.

Fig. 3. a) Absorption spectra of L (2.5μM) with varying Sn^{2+} concentration in THF– HEPES buffer (90:10, v/v, pH 7.4)   **b)** Fluorescence spectra of L (2.5μM) with varying Sn^{2+} concentration in THF– HEPES buffer (90:10, v/v, pH 7.4)

Fig. 4. Job plot (stoichiometric ratio) of L with Sn^{2+}

Fig. 5. Benesi-Hildebrand plot
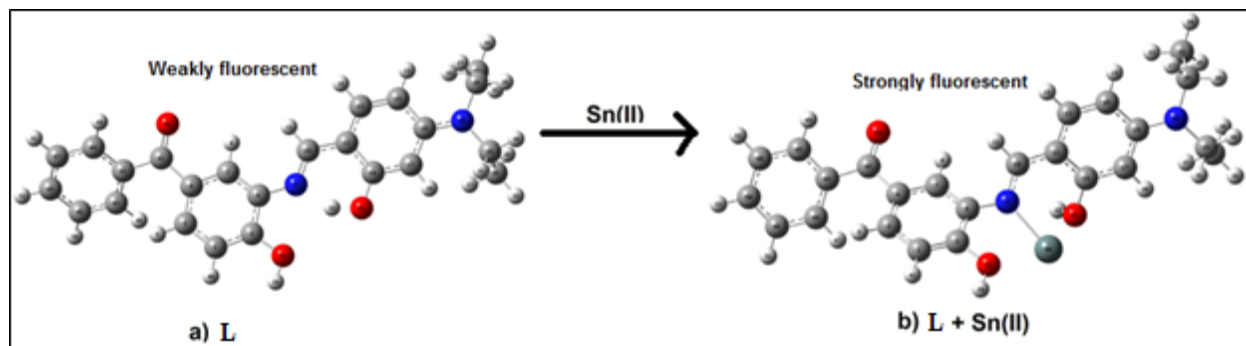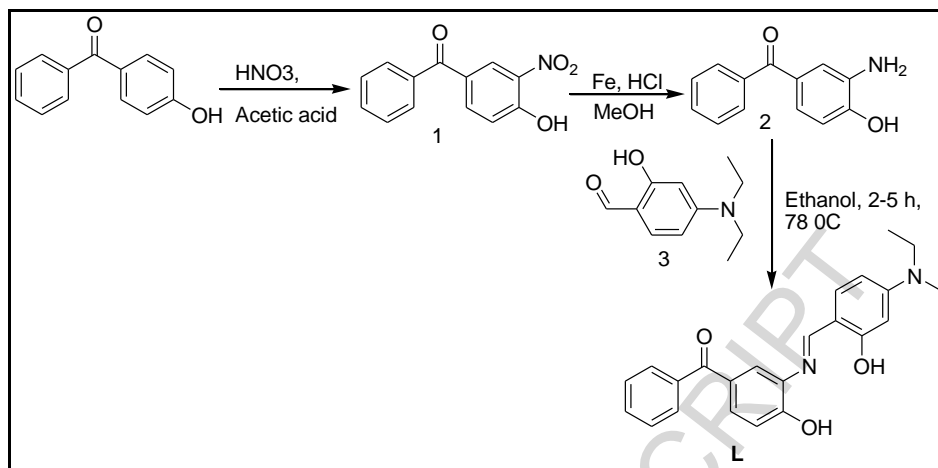
Fig. 6. Plot for detection limit calculation

Fig. 7. Comparative changes in ^{1}H NMR of L when binds with Sn^{2+}

Fig. 8. a) Optimized geometry of L at B3LYP/3-21g level. b) Optimized geometry of L- Sn^{2+} complex at B3LYP/3-21g level at gas phase.

Scheme1: Synthesis of (2-(2-hydroxyphenyl)-1H-benzo[d]imidazol-5-yl)(phenyl) methanone (**L**)

Tables

Table 1 Comparative selectivity, binding constant, detection limits with reported ligands

Table 2 Bond lengths of selected bonds

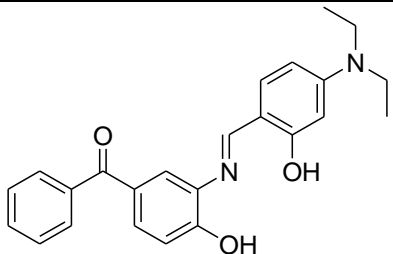**Table 1** Comparative selectivity, binding constant, detection limits with reported ligands

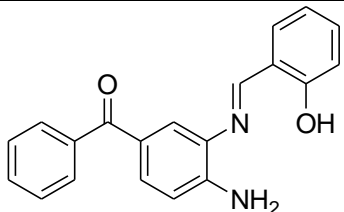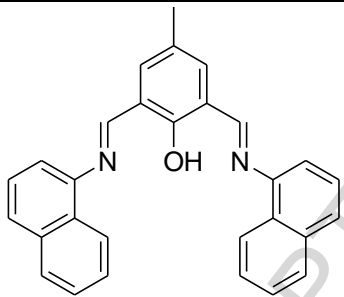| Sr. No.	Analyte (Ligand)	Sensivity/ Selectivity	Binding constant	Detection Limit	Reference
1		Sn^{2+}	$1.50 \times 10^4 \, M^{-1}$	0.3898 ppb	This work
2		Al^{3+}	$5.7 \times 10^3 \, M^{-1}$	0.0081 ppb	21
3		Sn^{2+} and Al^{3+}	$3.4 \times 10^5 \, M^{-1}$	2.72 ppb	23

Table 2 Bond lengths of selected bonds

Compound	C9=N10 (Å)	C14-O21 (Å)	C3-O23 (Å)	O21-H22 (Å)	O23-H24 (Å)
L	1.29379	1.37598	1.374	0.99423	0.99343
L+Sn(II)	1.3727	1.44143	1.3876	0.99606	0.99134

Graphical abstract
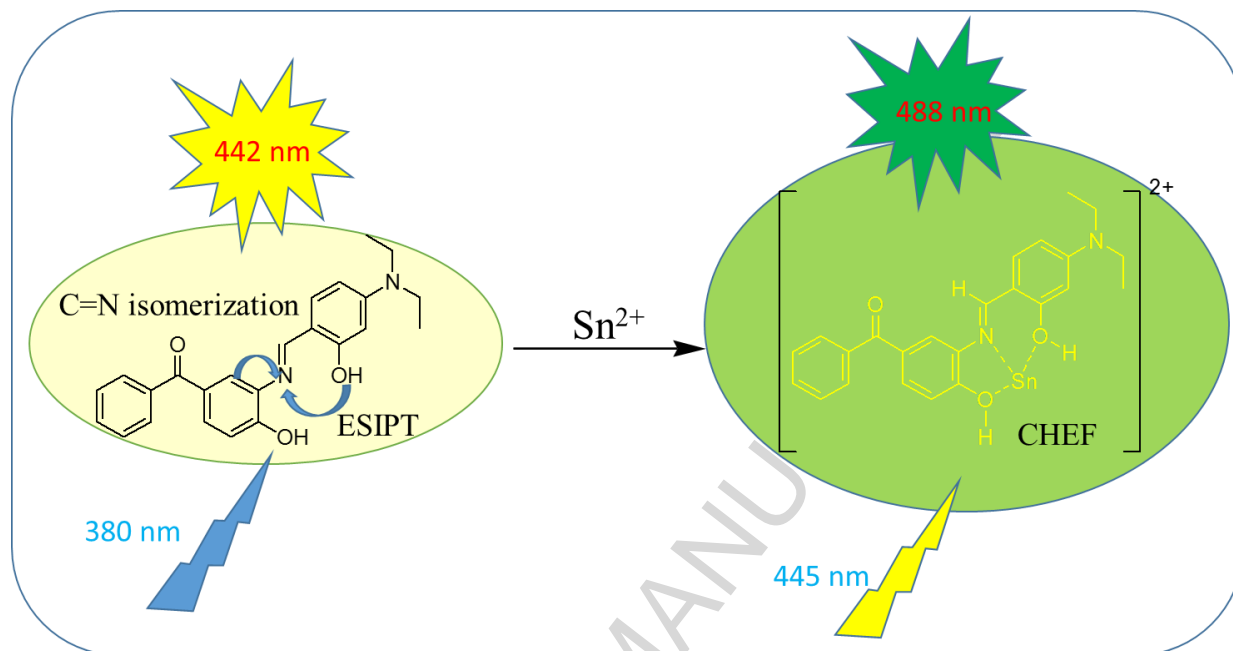
Highlights

➢ Simple novel benzophenone-based chemosensor has been synthesized for selective sensing of Sn^{2+} ion.

➢ Specific selectivity and superiority of our fluorophore over another recently and only reported fluorophore for Sn^{2+} ion sensing (along interference of Al^{3+}ion) is explained.

➢ The specific Sn^{2+} recognition was investigated by spectroscopic techniques and DFT study.

➢ Stoichiometric ratio, binding constant and LOD for complex is found to be 1:1 and 1.50 x 10^4 and 0.3898 ppb respectively.